Original Research

MR Pharmacokinetic Modeling of the Patellar Cartilage Differentiates Normal From Pathological Conditions

Roberto Sanz, MS,[1]* Luis Martí-Bonmatí, MD,[1,2] José Luis Rodrigo, MD,[2] and David Moratal, PhD[3]

Purpose: To study the pharmacokinetic parameters derived from dynamic contrast-enhanced magnetic resonance imaging (DCE-MRI) of the patellar cartilage under normal and pathological conditions.

Materials and Methods: DCE-MRI was obtained in 22 cases. There were 17 patients with degenerative patellar conditions (eight with chondromalacia and nine with osteoarthritis) and five normal subjects. The cartilage pharmacokinetic parameters of K^{trans} (vascular permeability), k_{ep} (extraction ratio), υ_e (extravascular extracellular space [EES] volume fraction), and υ_p (intravascular space volume fraction) were extracted.

Results: Statistically significant differences were observed between the different groups (normal cartilage, chondromalacia and osteoarthritis) for K^{trans} and υ_e. K^{trans} values were (mean ± SD) 1.06 ± 0.62, 11.97 ± 8.91, and 21.21 ± 16.03 mL · minute^{-1} · 100 mL^{-1} ($P < 0.02$), respectively; and υ_e values were 0.71 ± 0.69, 3.59 ± 2.21, and 10.51 ± 8.20% ($P < 0.002$). Reproducibility of the pharmacokinetic calculations was assessed with a second set of analyses of 10 random cases one week after the first analysis, showing a test-retest root mean square (RMS) coefficient of variation of 9.78% for K^{trans} and 14.72% for υ_e.

Conclusion: The vascular permeability and EES fraction of cartilage increases with the severity of the degeneration. Pharmacokinetic models allow to study the vascular properties of the cartilage and may have applications as a surrogate index in longitudinal studies to quantify the evolution of drug trials.

Key Words: cartilage; pharmacokinetic modeling; contrast-enhanced MRI; reproducibility; chondromalagia; osteoarthritis
J. Magn. Reson. Imaging 2008;27:171–177.

RECENT ADVANCES in the treatment of cartilage anomalies demand more imaging information to detect earlier lesions before they are severe enough. Degenerative osteoarthritis and chondromalacia are common diseases of the articular cartilage, affecting and disabling millions of people from their normal daily activity (1). Chondromalacia affects the main substance and the collagen fibers as well as the deeper regions of the cartilage. It tends to develop toward femoropatellar osteoarthritis. In osteoarthritis the water content in the cartilage increases and the collagen matrix stiffness decreases, leading toward mechanical overloads of the cartilage and destruction of tissue (2).

The standard method to quantify the cartilage degree of injury is arthroscopy with biopsy of the cartilage (1), which is an invasive and expensive technique. MRI allows the study of the cartilage with great detail, offering excellent spatial and contrast resolution. The use of dynamic contrast-enhanced MRI (DCE-MRI) can further increase our knowledge of the cartilage abnormalities by analyzing its vascularization and blood supply (1). Although the cartilage is often considered to be completely avascular, several studies have shown that there are vascular contacts both at the calcified and the uncalcified parts (3–8). These supplies run through tubular microstructures (channels) that start at the subchondral bone and cross the calcified cartilage into the basal regions of the cartilage (4,5).

Our hypothesis is that an increase in the capillarity parameters is associated with the severity of the cartilage degeneration. Therefore, the pharmacokinetic analysis of the cartilage may show significant differences between the different stages of articular degeneration.

Several approaches can be taken in the analysis of the patellar perfusion evaluation. A semiquantitative approach is the calculation of the arrival of the contrast bolus (upslope, maximum value, area under curve, time to 90%), measured from the signal intensity curve at the voxels of interest (3,9–12). Different uptakes observed in the patellar cartilage allows us to suppose that in disease states there are vascular changes in the deeper layers of the cartilage, characterized by an increase in upslope values (3). This semiquantitative ap-

[1]Radiology Department, Hospital Quirón, Valencia, Spain.
[2]Hospital Universitario Dr. Peset, Valencia, Spain.
[3]Electronic Engineering Department, Universitat Politècnica de València, Valencia, Spain.
Contract grant sponsor: Rottapharm S.L.
*Address reprint requests to: R.S.R., Servicio de Radiología – Hospital Quirón Valencia, Avda. Blasco Ibáñez 14, 46010 Valencia, Spain. E-mail: rsanz.val@quiron.es
Received May 10, 2007; Accepted September 24, 2007.
DOI 10.1002/jmri.21233
Published online 16 November 2007 in Wiley InterScience (www.interscience.wiley.com).

proach is simple and fast, but often lacks reproducibility and does not focus directly on the microvascular properties of the tissue and the extravascular extracellular space (EES). Pharmacokinetic modeling has been designed to offer complete reproducibility as it is less dependent of the equipment and patient under study. Two models based on the works by Tofts et al (12,13) are used and compared in this study: the original one and an extended model. Both offer information on the permeability between vessels and EES, K^{trans} (mL · minute^{-1} · 100 mL^{-1}); the extraction rate between EES and vessels, k_{ep} (mL · minute^{-1} · 100 mL^{-1}); and the EES volume fraction, υ_e (%). However, only the second model considers the intravascular volume fraction, υ_p (%).

Our interest was to study the pharmacokinetic parameters derived from DCE-MRI of the patellar cartilage under both normal and pathological conditions. We compared these parameters by implementing the pharmacokinetic model on a software developed at our laboratory. Reproducibility of the results was also assessed by performing a second analysis one week after the first set of measurements.

MATERIALS AND METHODS

Patients and Data Acquisition

A total of 25 patients who underwent a DCE-MRI of the knee were initially included in the study. A total of three patients were withdrawn because of patient's movement during the MR acquisition, leaving five healthy subjects and 17 patients with degenerative patellar conditions (eight with chondromalacia and nine with osteoarthritis). Normal subjects and patients with chondromalacia were similar (43.6 ± 15 and 33.3 ± 11.8 years old, respectively) but younger than patients with osteoarthritis (58.9 ± 11.5 years old) ($P = 0.002$). Regarding gender, there were 14 women (three normal, seven with chondromalacia, and four with osteoarthritis) and eight men (two normal, one with chondromalacia, and five with osteoarthritis).

MRI was performed on a 1.5T magnet (Philips Gyroscan Intera; Philips Medical Systems, Best, The Netherlands). A T_1-weighted contrast-enhanced spoiled gradient echo was acquired with the following parameters: TR = 3.47 msec, TE = 1.93 msec, flip angle = 10°, reconstruction matrix size = 256 × 256, pixel size = 0.78 × 0.78 mm, and slice thickness = 10 mm. Each dynamic comprised 10 slices and the sequence had 50 time points, each one with a temporal resolution of 2.9 seconds. The total acquisition time was two minutes and 25 seconds.

An intravenous contrast agent (Gd-DTPA-BMA, Omniscan®; GE Healthcare, UK) was injected as a bolus (0.2 mL/kg at 4 mL/second), followed by a 40-mL saline flush at the same rate.

Pharmacokinetic Modeling

In this work a one-input two-compartment model was used. The popliteal artery signal enhancement curve was used as the arterial input function (AIF) to the model, being the two compartments the blood plasma and the EES.

The mathematical expression that governs the evolution of contrast agent concentration in the tissue is the following convolution equation identified as the original Tofts et al (12) model:

$$C_t(t) = K^{\text{trans}} \int_0^t C_p(u) e^{-k_{ep}(t-u)} du, \qquad (1)$$

where C_t is the contrast agent concentration in the EES of the cartilage and C_p is the contrast agent concentration in the popliteal artery. υ_e is related to K^{trans} and k_{ep} with the following expression: $\upsilon_e = K^{trans}/k_{ep}$. The physiological sense of υ_e sets its range from 0% to 100% (12).

The extended Tofts et al (12) model considers the vascular contribution to the concentration of contrast in the EES and was written as:

$$C_t(t) = \upsilon_p C_p(t) + K^{\text{trans}} \int_0^t C_p(u) e^{-k_{ep}(t-u)} du. \qquad (2)$$

Although the original Tofts et al (12) model may produce an overestimation of the parameters K^{trans} and υ_e (9–14), it may be appropriate in those situations where the vascular contribution may be neglected, as in normal or weakly irrigated tissues like the cartilage (12). To assess these differences, we used and compared both models in this study.

As the model formulation is based on concentration, the intensity vs. time curves were converted into concentration vs. time curves. Assuming that $TR \cdot r_1 \cdot C_t << 1$, $TE \cdot r_2 \cdot C_t << 1$, and $TR << T_{10}$ (where TR is the repetition time, r_1 is the longitudinal relaxivity, r_2 is the transversal relaxivity, and T_{10} is the T_1 before contrast administration), the normalized intensity vs. time curve can be linearly related to the contrast agent concentration (15):

$$\frac{S_t(t)}{S_0} - 1 \approx T_{10} \cdot r_1 \cdot C_t(t), \qquad (4)$$

where $S_t(t)$ is the intensity vs. time curve and S_0 is the signal intensity before contrast agent administration. This approach seems valid as our case complies with the previous conditions for the heaviest patient in our sample (100 kg body weight),

- $TR \cdot r_1 \cdot C_t \leq 3.47$ msec · 4.5 mM^{-1} second^{-1} · 0.2 mL/kg · 100 kg · 0.5 mM/mL = 0.2 << 1 (assuming maximum concentration)
- $TE \cdot r_2 \cdot C_t \leq 1.93$ msec · 5.5 mM^{-1}second^{-1} · 0.2 mL/kg · 100 kg · 0.5 mM/mL = 0.1 << 1 (assuming maximum concentration)
- $TR << T_{10} \approx 1$ second (15,16)

The resulting concentration curves for the AIF and each pixel are used in Eqs. [1] and [2]. To calculate the pharmacokinetic parameters, a nonlinear least square

fit using the Levenberg-Marquardt (17) method was performed, a method that has been proved to be robust and fast.

Image Analysis

A region of interest (ROI) containing the cartilage was defined by manually drawing the cartilage in the precontrast image of the transverse slice through the largest left-right patellar diameter. The AIF was taken from a ROI drawn within the popliteal artery (see Fig. 1). All the pixels within the arterial ROI were averaged at every time point. No further function, apart from pixel averaging and moving averages, was used to smooth the contrast enhanced curves. The pixel-by-pixel pharmacokinetic analysis of the cartilage was averaged to obtain the mean cartilage values. As the knee was tightly immobilized, image registration was not considered necessary. All intensity curves were normalized before intensity to concentration conversion.

The pharmacokinetic analysis was performed on pixels defined as enhanced on the manual ROI. Only pixels which enhanced, defined as three SDs higher than the base image before contrast administration (9) were computed. Enhanced pixels were sieved, and those with υ_e values higher than 100% were discharged according to the physiological criteria established by Tofts et al (12).

Enhanced pixels, as defined above, were counted and their pharmacokinetic parameters were calculated. Parametric colored maps were overlapped over anatomical slices, obtaining color-coded parametric images. All this computational and graphic analysis was implemented in Matlab 7.3 (R2006b; The Mathworks, Inc., Natick, MA, USA) running on a PC (Pentium 4 at 2.8 GHz and 2.5 GB of RAM memory).

Statistical Analysis

Statistical analysis was performed with the SPSS 13.0 for Windows (SPSS, Inc., Chicago, IL, USA). A one-way analysis of variance (ANOVA) test was performed with a P value <0.05 considered to be statistically significant. For the test-retest analysis of variability the root mean square (RMS) coefficient of variation was calculated:

$$RMS\_CoV = \sqrt{\frac{\sum_{i=1}^{N}\left(\frac{\sigma_i}{\mu_i}\right)^2}{N}}, \qquad (6)$$

where σ_i is the SD and μ_i the mean of each pair of measurements and $N = 10$ cases. The 10 patients selected for the variability analysis were randomly chosen (two normal, three with chondromalacia and five with osteoarthritis). Low values of RMS coefficient of variance (CoV) correspond to a high reproducibility of the results. The number of pixels with enhancement was analyzed with the ANOVA test with multiple comparisons by using the Student-Newman-Keuls test, performed at the 5% level of significance.

All the results are expressed as mean ± SD.

RESULTS

Pharmacokinetic Analysis

In the comparison between the three cartilage status groups, the original Tofts et al (12) model showed significant differences for K^{trans} and υ_e, with P values of 0.012 and 0.001, respectively. k_{ep} was not significantly different ($P = 0.884$). For the extended Tofts et al (12) model, significant P values were also obtained for K^{trans} and υ_e ($P = 0.02$ and $P = 0.007$, respectively), but not for k_{ep} and υ_p (P values of 0.897 and 0.379, respectively).

Computing time was not critical in any of the two models, basically because the amount of pixels to be analyzed was not high (generally less than half a minute per study, a few hundreds of pixels with a speed of 90 ± 60 [mean ± SD] msec per pixel). However, the computational burden associated with each model was clearly different because of the one extra free parameter to fit with the extended method (50 ± 10 msec per pixel for the original model and 130 ± 60 msec per pixel for the extended model).

Table 1 summarizes the values of the parameters obtained for each model, while Fig. 2 shows the plots for the K^{trans} and υ_e statistic values in the first model, which showed the best significance. Finally, Fig. 3 shows K^{trans} parametric maps for a normal cartilage and a cartilage with osteoarthritis.

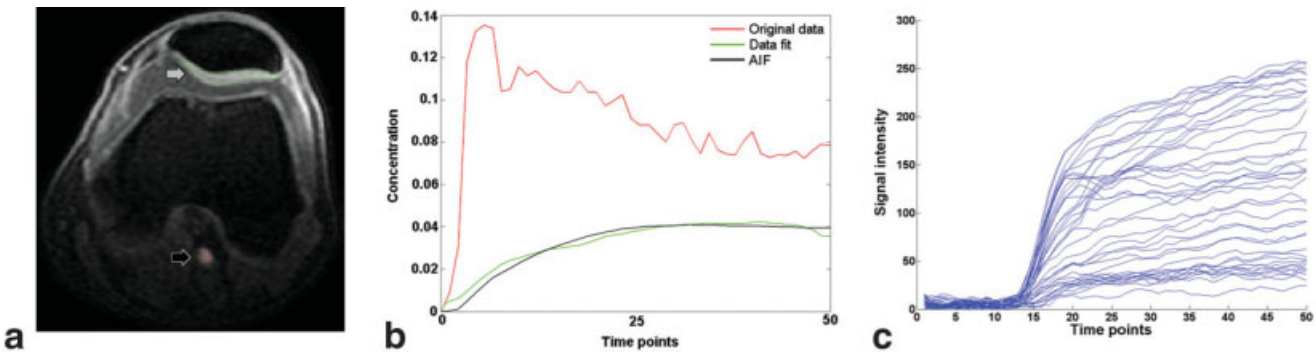

Figure 1. a: DCE-MRI slice showing the regions of interest for the cartilage (gray arrow) and the popliteal artery (black arrow). **b:** Concentration enhancement for the artery (red) and for an arbitrary cartilage pixel (green). The fit data curve is shown in black. **c:** Normalized enhancement evolution of all the pixels pertaining to the cartilage ROI. [Color figure can be viewed in the online issue, which is available at www.interscience.wiley.com.]

Table 1
Summary of Results (Mean ± SD) for the Pharmacokinetic Parameters in Both Proposed Models

Model	Parameter[a]	Pathology			*P*
		Normal	Chondromalacia	Osteoarthritis	
Original Tofts	K^{trans}	1.06 ± 0.62	11.97 ± 8.91	21.21 ± 16.03	0.012
	k_{ep}	313.21 ± 40.35	279.64 ± 161.09	273.48 ± 140.97	0.893
	υ_e	0.71 ± 0.69	3.59 ± 2.21	10.51 ± 8.2	0.001
Extended Tofts	K^{trans}	0.19 ± 0.47	7.68 ± 6.26	13.24 ± 10.89	0.021
	k_{ep}	352.3 ± 54.63	311.69 ± 149.71	321.08 ± 173	0.894
	υ_e	0.69 ± 0.28	3.68 ± 2.57	10.11 ± 9.05	0.007
	υ_p	0.49 ± 0.14	0.59 ± 0.58	1.3 ± 2.2	0.381

[a]Units: K^{trans} (mL·minute^{-1}·100 mL^{-1}), k_{ep} (mL·minute^{-1}·100 mL^{-1}), υ_e (%, no units), and υ_p (%, no units).

Reproducibility Analysis

A total of 10 of the 22 MR examinations were analyzed twice, the second time seven days after the first analysis. To avoid the variations due to different selection of the slices, the same centered slice was selected for the pharmacokinetic analysis. The popliteal artery and the full thickness cartilage were again manually drawn by the same researcher with ROIs. Except for the RMS CoV for υ_p, the other values of reproducibility were good or very good (10) (range = 8–19%), with k_{ep} being the most reproducible parameter in both models (Table 2).

Enhancement Extension Analysis

Significant differences were observed in the number of enhanced pixels between the normal subjects and the other two groups (P = 0.001). However, although no significant differences were obtained between chondromalacia and osteoarthritis patients, a tendency could be observed towards a greater enhancement of the osteoarthritis group. For the normal subjects, the number of enhanced pixels was 45 ± 12.9; for the chondromalacia group, it was 66.4 ± 41.2; and for the osteoarthritis group, it was 82.6 ± 39.8. Figure 4 shows the statistical gap between normal and diseased patella.

DISCUSSION

Many studies in the last few years have focused on the use of MR pharmacokinetic models to detect and discriminate pathological states and grades in different diseases. Patellar cartilage has not been an important focus of attention for this type of analysis, probably due to its low perfusion and the limitations of MR in the spatial and temporal resolutions. However, some studies point to a correlation between articular cartilage degeneration and the presence of an abnormality in its blood supply and nutrition (3,7).

Our study seems to be one of the first evaluations of the perfusion and pharmacokinetic characteristics of the synovial articular cartilage, both in the normal and disease status. Our results show a good correlation

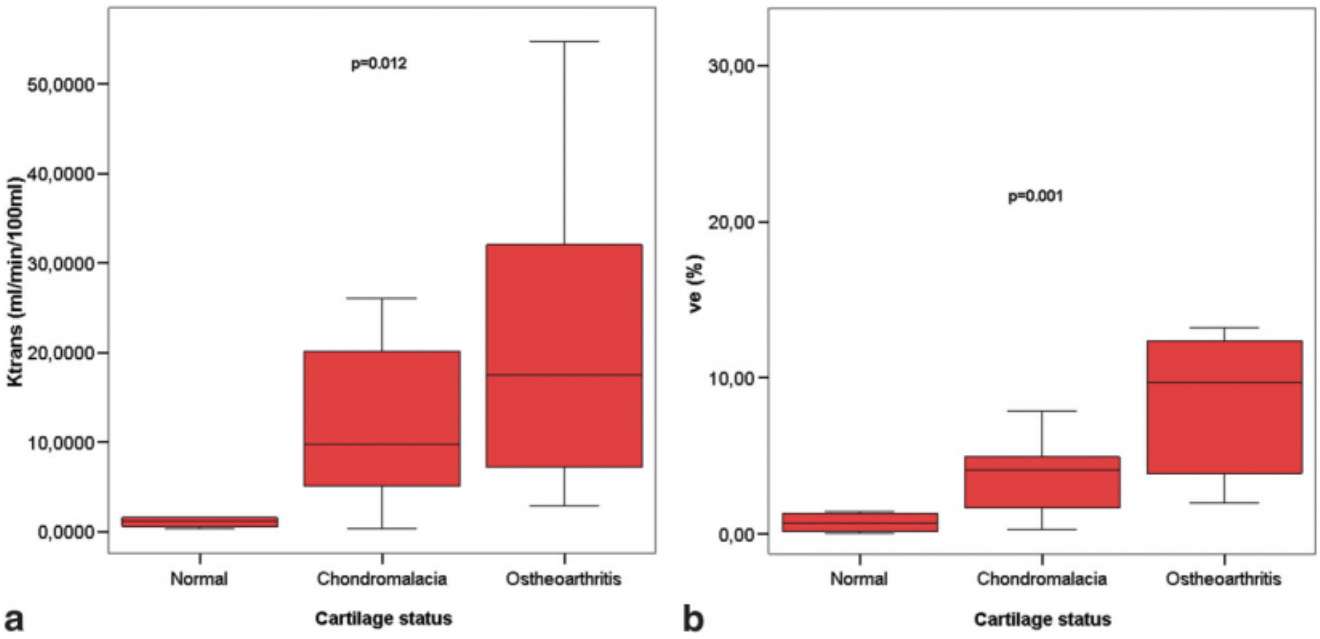

Figure 2. Box-plots for (**a**) K^{trans} and (**b**) υ_e. Both parameters are obtained using the Tofts et al (12)standard method (dismisses the vascular contribution). The chart shows the five statistics (minimum, first quartile, median, third quartile, and maximum). [Color figure can be viewed in the online issue, which is available at www.interscience.wiley.com.]

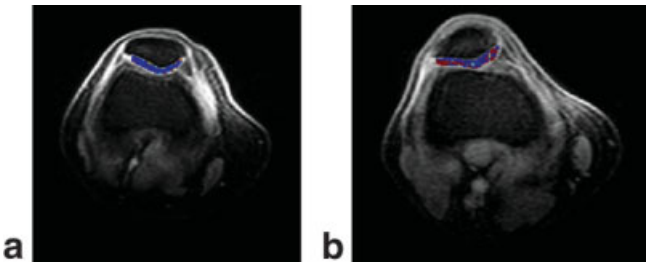

Figure 3. Cartilage parametric maps for K^{trans}: (**a**) shows a normal cartilage; (**b**) shows a cartilage with osteoarthritis. Blue and green represent lower values. Yellow and red represent higher values.

with the initial hypothesis. The DCE-MRI quantification by pharmacokinetic analysis shows a significant difference in the K^{trans} and υ_e between normal cartilage and cartilage affected by chondromalacia and osteoarthritis. The values obtained for K^{trans} and υ_e show a surrogate index of an increase of microvascularity and interstitial volume as the cartilage degenerates to more advanced stages. Also, the analysis of the number of pixels with enhancement shows a higher abnormal pixel recruitment in osteoarthritis than in chondromalacia, and much higher in both than in the normal cartilage group. This clearly correlates with the extension of the abnormality, described as enhanced pixels, present in more advanced stages of cartilage degeneration and osteoarthritis.

We have also demonstrated that the results obtained considering or not the vascular contribution (υ_p parameter) are different, in agreement with the hypothesis of the Tofts et al (12)original model. If the vascular contribution υ_p is dismissed, K^{trans} and υ_e values increase (14). This difference in the measurements is bigger as the degeneration of the cartilage increases, due to a more advanced grade of angiogenesis. From our experience, we propose to consider $\upsilon_p = 0$ to increase the curves' goodness of fit, the reproducibility, and the stability of the model. This will also decrease unnecessary complexity, and enlarge the statistical difference between cartilage disease states.

In this sense, methodological reproducibility is a must with a new quantification tool. We have demonstrated that the pharmacokinetic variables have, globally, good reproducibility. The only exception is the quantification of the vascular volume fraction (υ_p), therefore limiting its use in clinical evaluations. Even more, these good reproducibility results are slightly better when the vascular contribution υ_p is dismissed (variation of 10% and 13% for K^{trans}, and 15% and 19% for υ_e, for not using υ_p vs. using υ_p, respectively). Neglecting υ_p, our results are quite in agreement with those obtained for brain data by Jackson et al (10), where K^{trans} and υ_e appeared to have excellent reproducibility (coefficient of variation of 8% and 6% for K^{trans} and υ_e, respectively), as in the study of Roberts et al (9) (8% and 15% for K^{trans} and υ_e, respectively). We found that k_{ep} values have an excellent reproducibility but unfortunately they do not show differences to be used in cartilage tissue characterization. In longitudinal studies for drug trials, DCE-MRI pharmacokinetic analysis could be used to measure the effectiveness of the treatment as the reproducibility of the methods is properly assessed.

Pharmacokinetic analysis from DCE-MRI may be applied to any tissue with perfusion. Its potentiality remains in modeling the vascular and interstitial behavior of different pathological conditions. The obtained pharmacokinetic parameters are expected to be reproducible between different laboratories, as long as similar sequences and measurement procedures are used. However, many issues must be taken into account and further investigated to minimize reproducibility problems (9–11,14,18). Therefore, several bias must be considered. The conversion from signal intensity to concentration curves, which has several steps and approximations, can be done with different methods as the use of linear conversion, polynomial conversion (19) or T_1 calculated maps (9,10,20,21). A relatively low temporal resolution may be a critical factor if the AIF peak is not correctly sampled, leading to underestimation of the exponential decay of the curve. The contrast injection rate affects the shape of the curves and therefore the calculated parameters. Image registration was not considered in our series as the knee does not move ostensibly, although some minor movement may account for dispersion of the calculated data. The consideration of the vascular contribution to the total concentration of the tissue (modeled by υ_p) may affect calculations in tissues with high grades of angiogenesis, which is not the case in the cartilage. Also, the variations in the MR sequence may influence the final results (22). Finally, the AIF selection may also produce differences in the results, depending on whether it is chosen for each individual, for a whole group as a mean, or from reference from other studies. At present, all these technical limitations make pharmacokinetic

Table 2
Reproducibility Results Obtained From a Test-Rest Root Mean Squared Coefficient of Variance (RMS CoV) for 10 Random Patients in Both Proposed Models

Model	Parameter[a]	Difference (mean ± SD)	% Difference (mean ± SD)	RMS CoV
Original Tofts	K^{trans}	1.17 ± 1.36	9.15 ± 10.29	0.0978
	k_{ep}	14.88 ± 5.61	10.23 ± 4.89	0.0815
	υ_e	1.16 ± 1	17.1 ± 18.26	0.1472
Extended Tofts	K^{trans}	1.52 ± 1.33	13.81 ± 10.86	0.1281
	k_{ep}	17.45 ± 12.2	10.17 ± 7.48	0.0920
	υ_e	1.75 ± 1.21	23.71 ± 24.08	0.1899
	υ_p	0.08 ± 0.08	46.48 ± 58.46	2.6208

[a]Units: K^{trans} (mL · minute^{-1} · 100 mL^{-1}), k_{ep} (mL · minute^{-1} · 100 mL^{-1}), υ_e (%, no units) and υ_p (%, no units).

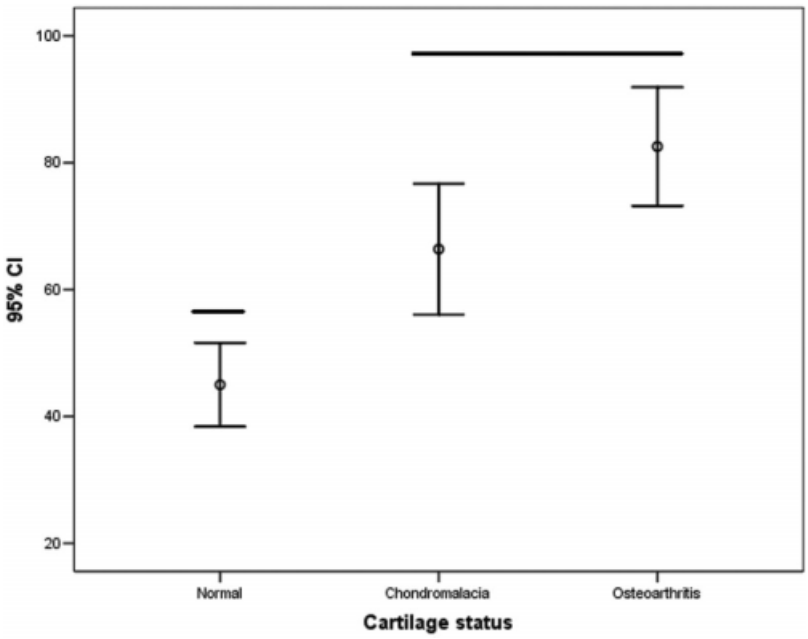

Figure 4. Plot showing mean ± 95% confidence interval (CI) for enhanced pixels on the three groups: normal, chondromalacia, and osteoarthritis. Significant differences were observed between the normal and the disease groups. No significant difference was observed between the chondromalacia and the osteoarthritis group (continuous line).

models a complex method, with more uncertainty than the model-free semiquantitative methods (i.e., measurements of upslope, area under curve, or time to 90% of the maximum intensity). However, these models can offer a different type of information, as they focus directly on the tissue microvascular function, providing a reliable and reproducible measurement of angiogenesis, if properly controlled.

In this study, several assumptions regarding pharmacokinetics were made. Cartilage has a low perfusion, there is a linear conversion between intensity and concentration, a direct use of the concentration curves can be employed without mathematical exponential approximation (15,23), and there is no need for dynamic image registration. Moreover, only the widest patella transverse slice image is analyzed in each patient to improve the quality of the manual segmentation of cartilage. Although this single analysis may be representative of the cartilage general state, a more detailed study should comprise the analysis of the whole cartilage to avoid missing nonregular distributions of the disease. Regarding the AIF selection, we decided to use individual manually defined AIFs as the popliteal artery was shown with clear margins due to the sufficient spatial resolution of the images and also because the peak enhancement was always present in all the cases due to the good temporal resolution of the sequence. However, a further study taking into account a mean AIF from the whole group to minimized individual variability would be interesting. Also, we must consider the bias of not having pathological proof of the normal cartilage and of some cases with degeneration. However, the strong relationship between the cartilage condition and the increase in the vascular permeability and EES (K^{trans} and υ_e) allows them to be used as surrogate markers of cartilage degeneration.

In conclusion, we have demonstrated that the pharmacokinetic analysis of the patellar cartilage presents statistical difference in the capillary permeability and interstitial component between normal and disease status. Even more, these abnormalities are higher with more diseased stages. Therefore, it seems reasonable to study higher number of patients for a better assessment of this pharmacokinetic models in the detection and grading of synovial cartilage disease.

REFERENCES

1. Gold GE, McCauley TR, Gray ML, Disler DG. What's new in cartilage? Radiographics 2003;23:1227–1242.
2. Waldschmidt JG, Rilling RJ, Kajdacsy-Balla AA, Boynton MD, Erickson SJ. In vitro and in vivo MR imaging of hyaline cartilage: zonal anatomy, imaging pitfalls, and pathologic conditions. Radiographics 1997;17:1387–1402.
3. Martí-Bonmatí L, Montaner D, Sanfeliu M. Análisis de la perfusión del cartílago rotuliano mediante resonancia magnética dinámica: aplicación en sujetos con dolor anterior de origen rotuliano. [An analysis of patellar cartilage perfusion by dynamic magnetic resonance: its application to subjects with anterior pain of patellar origin]. Rev Clin Esp 1999;199:641–646.
4. Imhof H, Breitenseher M, Kainberger F, Rand T, Trattnig S. Importance of subchondral bone to articular cartilage in health and disease. Top Magn Reson Imaging 1999;10:180–192.
5. Imhof H, Sulzbacher I, Grampp S, Czerny C, Youssefzadeh S, Kainberger F. Subchondral bone and cartilage disease: a rediscovered functional unit. Invest Radiol 2000;35:581–588.
6. Graf J, Fromm B, Schneider U, et al. The application of the plastination method in experimental orthopaedic surgery. J Int Soc Plastination 1991;5:20–22.
7. Slater RNS, Spencer JD, Churchill MA, Bridgeman GP, Brookes M. Observations on the intrinsic blood supply to the human patella: disruption correlated with articular surface degeneration. J R Soc Med 1991;84:606–607.
8. Bashir A, Gray ML, Boutin RD, Burstein D. Glycosaminoglycan in articular cartilage: in vivo assessment with delayed $Gd(DTPA)^{2-}$-enhanced MR imaging. Radiology 1997;205:551–558.
9. Roberts C, Issa B, Stone A, Jackson A, Waterton JC, Parker JM. Comparative study into the robustness of compartmental modeling and model-free analysis in DCE-MRI studies. J Magn Reson Imaging 2006;23:554–563.
10. Jackson A, Jayson GC, Li KL, et al. Reproducibility of quantitative dynamic contrast-enhanced MRI in newly presenting glioma. Br J Radiol 2003;76:153–162.

11. Padhani AR. Dynamic contrast-enhanced MRI in clinical oncology: current status and future directions. J Magn Reson Imaging 2002; 16:407–422.
12. Tofts PS, Brix G, Buckley DL, et al. Estimating kinetic parameters from dynamic contrast-enhanced T_1-weighted MRI of a diffusable tracer: standardized quantities and symbols. J Magn Reson Imaging 1999;10:223–232.
13. Tofts PS. Modeling tracer kinetics in dynamic Gd-DTPA MR imaging. J Magn Reson Imaging 1997;7:91–101.
14. Buckley DL. Uncertainty in the analysis of tracer kinetics using dynamic contrast-enhanced T_1-weighted MRI. Magn Reson Med 2002;47:601–606.
15. Workie DW, Dardzinski BJ. Quantifying dynamic contrast-enhanced MRI of the knee in children with juvenile rheumatoid arthritis using an arterial input function (AIF) extracted from popliteal artery enhancement, and the effect of the choice of the AIF on the kinetic parameters. Magn Reson Med 2005;54:560–568.
16. Gold GE, Han E, Stainsby J, Wright G, Brittain J, Beaulieu C. Muskuloskeletal MRI at 3.0 T: relaxation times and image contrast. AJR Am J Roentgenol 2004;183:343–351.
17. Marquardt D. An algorithm for least squares estimation of nonlinear parameters. J Soc Indust Appl Math 1963;11:431–441.
18. Padhani AR, Hayes C, Landau S, Leach MO. Reproducibility of quantitative dynamic MRI of normal human tissues. NMR Biomed 2002;15:143–153.
19. Materne R, Smith AM, Peeters F, et al. Assessment of hepatic perfusion parameters with dynamic MRI. Magn Reson Med 2002; 47:135–142.
20. D'Arcy JA, Collins DJ, Padhani AR, Walker-Samuel S, Suckling J, Leach MO. Magnetic resonance imaging workbench: analysis and visualization of dynamic contrast-enhanced MR imaging data. Radiographics 2006;26:621–632.
21. Armitage P, Behrenbruch C, Brady M, Moore N. Extracting and visualizing physiological parameters using dynamic contrast-enhanced magnetic resonance imaging of breast. Med Image Anal 2005;9:315–329.
22. Evelhoch JL. Key factors in the acquisition of contrast kinetic data for oncology. J Magn Reson Imaging 1999;10:254–259.
23. Horsfield MA, Morgan B. Algorithms for calculation of kinetic parameters from T1-weighted dynamic contrast-enhanced magnetic resonance imaging. J Magn Reson Imaging 2004;20:723–729.